Acta Polytechnica **63**(1):23–35, 2023
https://doi.org/10.14311/AP.2023.63.0023

Published by the Czech Technical University in Prague

SELF-INTERFERENCE CANCELLATION IN UNDERWATER ACOUSTIC COMMUNICATIONS SYSTEMS USING ORTHOGONAL PILOTS IN IBFD

Hala A. Naman[a,b], Ammar E. Abdelkareem[a,*]

[a] *Al-Nahrain University, College of Information Engineering, Department of computer Networks Engineering, Baghdad, Iraq*

[b] *University of Wasit, College of Engineering, Department of Architecture, Wasit, Iraq*

[*] corresponding author: Ammar.algassab@nahrainuniv.edu.iq

Abstract. This paper proposes a Self-interference (SI) cancellation system model of Underwater acoustic (UWA) communication for in-band full-duplex (IBFD) technology. The SI channel is separated from the Far channel by exploiting a concurrently orthogonal pilot channel estimation technique using two orthogonal frequency-division multiplexing (OFDM) blocks to establish orthogonality between them based on a unitary matrix. Compared to the half-duplex channel estimator, the mean squared error (MSE) and the bit error rate (BER) provided strong evidence for the efficiency of the proposed SI cancellation. Since full-duplex systems are more efficient than half-duplex ones, the proposed approach might be seen as a viable option for them. The proposed method proved effective when used with a fixed full-duplex (FD) position and FD shifting of up to 4°. Different channel lengths and distances are adopted to evaluate the proposed method. Initial findings indicate that MSE for the SI channel minimum mean-square error (MMSE) estimator at 20 dB is $0.118 \cdot 10^{-3}$, for fixed FD. In addition, this paper presents a geometry channel model for the Far channel in the IBFD underwater communication system that describes the propagation delay of the multipath reflection. The simulation results for the multipath propagation delay spread are similar to the traditional results, with the delay spread of the suggested model reaching (79 ms), which is close to the Bellhop simulator result (78 ms).

Keywords: Full duplex, self-interference cancellation, Far channel model, channel estimation, multipath propagation, underwater acoustic communication.

1. Introduction

Many industries have found a use for the UWA communication technology, which has been extensively researched and put into practice in areas including underwater sensor networks, marine environment observation, oceanographic engineering building, etc. [1]. UWA communication systems' spectral efficiency is limited by three variables: the small frequency bandwidth available, the complexity of UWA multipath propagation, and the slow speed of sound underwater ($1500\,\mathrm{m\,s^{-1}}$) [2, 3]. To maximise the usage of the radio spectrum, the FD communication technology was developed [4, 5]. This technology may also be applied to UWA communications systems. Many studies have been done on the viability of FD technology in UWA communication systems [6, 7], particularly the IBFD technology, due to its ability to increase system performance by a factor of two by doubling the frequency spectrum efficiency. Due to the signal of the near transmitter in FD interfering with the signal of interest from the far transmitter and preventing the receiver of FD from detecting the desired signal because of its high power and long delay spread of multipath propagation, the SI cancellation is a primary challenge regarding FD communications and has been the primary focus of research efforts. The SI cancellation may be realised in two ways: analog cancellation and digital cancellation. The SI cancellation performance can be enhanced by obtaining more precise SI and Far channel estimations [8, 9]. To reach an excellent estimation, we should be able to distinguish between the SI and the Far channel at the reception. This separation may be attained using orthogonality, which is employed in the transmission techniques of OFDM that operate in a half-duplex mode. Signals orthogonal to one another do not interact, conflict with one another, and can be examined individually without the other affecting the results. In order to estimate the SI and communication channel, it is common practice to employ a known pilot sequence; alternatively, it is recommended to use an orthogonal sequence as a pilot sequence. In this work, we assume that the corresponding positions of both the transmitter and the receiver are fixed. According to a research on SI channel characteristics, it is safe to deduce that the rapid channel fluctuations and the long SI channel reflections are the most crucial factors to take into account when developing a digital SI canceller.

2. Related works

In this section, we cover the literature on communication channel models for multipath propagation and self-interference cancellation methods in full-duplex transmissions. The suggested approach advances a previous research by maximising the precision of channel estimates while reducing unnecessary overhead.

In [10], the researchers suggested a model based on a binomial expression to describe the propagation delay of channel geometry for four types of multipath reflection based on the height difference between the transmitter and the receiver and the distance between them. They demonstrated that the attenuation coefficient would impact the system's efficiency when there is a significant height difference between the transmitter and receiver. In [11], a geometrical channel model for the propagation delay of multipath scattering based on the angles of departure and arrival in UWA communication was introduced. The researchers pretend that the multipath scatterers are spread out on the ocean surface and floor. In [12], a non-stationary wideband channel model in shallow water environments is proposed based on the angles of departure and angle of arrival. The researchers demonstrated that the suggested model was realistic and effective in enabling extended time/distance simulations because it takes into account numerous motion effects, such as time-varying angles, distances, and clusters' positions with the channel geometry caused by various motion factors that impact UWA channels. In [13], researchers offered a geometry model describing the propagation range and delay for direct and multipath reflected from surface and bottom in a tank environment with taking into account chemical constituents of water and sodium chloride with other factors of attenuation. They demonstrated that the transmission in the tank is substantially strong due to the enclosed space and the reflections from the tank wall and the surface and floor. Based on the previous literature, the previous models suffered from the complexity in geometry models and the direction of communication between the transmitter and the recipient is required to be in the horizontal direction only. In [14], researchers presented a digital SIC based on Non-parametric-Maximum-likelihood (NPML) with a sparse constraints approach to estimate the SI channel considering OFDM intended signal after Peak-to-Average Power ratio (PAPR) treated as non-Gaussian noise. The suggested method outperformed both standard NPML and LS in simulations and experiments, with a quicker convergence rate, more accurate SI channel estimate, and superior SI cancelation performance. In [15], researchers suggested a digital RF SIC system model of a transmitter and two receivers within the same equipment, used to collect a copy of the transmitted signal, which is then subtracted from the signal at the primary receiver. A Kalman filter is derived to estimate the correlated main channel and the auxiliary channel of both receivers in the presence of two forms of noise. In [16], researchers offered an SIC system model in Co-time Co-frequency FD (CCFD) UWA communication. To improve the performance of digital SIC by using the reconstructed SI signal from the SI channel obtained using an adaptive filter, they suggested using the SI signal combined with the intended signal in the estimation of the SI channel. In [17], an SIC model to estimate the SI and communication channels concurrently across a FD connection utilising orthogonal pilot sequences was proposed. The HD and FD of both channel estimators using the Cramer-Rao Lower Bound were compared. The estimators' effectiveness depends on the sequence length and number of channel taps. Maintaining sequence orthogonality and synchronisation through correlation characteristics is crucial to the efficacy of channel estimators. Both channel estimators are impacted by the cross-correlation deviation, whose sequences that are not synchronised at the receiver will determine the impact on the performance. The results also indicated a degradation of the estimator's performance with increasing channel length. Additionally, most existing works suffer from overhead and complexity caused by iterations of an adaptive filter; also, any small error in SI residual will affect the SIC performance.

Below is a description of the paper's contribution. We proposed a system model that can eliminate self-interference signal in the digital domain in an FD configuration by separating the Self signal from the Far signal without needing a complex overhead adaptive filter. The proposed system for cancelling self-interference employs two orthogonal OFDM blocks by creating an orthogonality between the Self signal and the Far signal, resulting in the complete separation of the two signals, proved mathematically, and the complete cancelation of self-interference. The proposed model does not depend on the channel length or the tap number of the channel impulse response and also applied efficiency with fixed FD and shifted FD. Additionally, we proposed a simple geometrical model for the Far channel based on a triangle to describe the multipath propagation of shallow underwater acoustic communication. The suggested model provides flexibility to the direction between the transmitter and receiver and consists of the direct path, multipath propagated by reflections on the sea surface, and multipath propagated by reflections on the sea floor. The outline for this paper is as follows: In Section 3, we dissect the proposed system model for channel model and SI cancellation. The simulation results and discussion are described in Section 4. Section 5 offers a summary of the paper.

3. System model

In this section, we introduce the architecture of the SIC model for the IBFD-UWA communication system along with the channel model, including both SI and Far channels and the measurements.

3.1. Structure of both transmitters

This work explores a scenario in which two UWA nodes communicate in IBFD mode where the Far node is a transmitter, and the Self node is a receiver. OFDM is used with quadrature phase shift keying (QPSK) modulation method with $\boldsymbol{N}$ subcarriers and equispaced comb-type pilot patterns for channel estimation with data index $\boldsymbol{d}$ and pilot index $\boldsymbol{p}$. The OFDM block $\boldsymbol{x}$ has been obtained by IFFT of baseband transmitted signal $\boldsymbol{X}$, which contains data and pilot subcarriers.

$$x = \text{IFFT}\{X\} = \frac{1}{N}\sum_{k=0}^{N-1} X[k] \exp\left(\frac{-j2\pi kn}{N}\right) \tag{1}$$

For each OFDM block, the cyclic prefix selected of length longer than the propagation of the excessive delay of the impulse response has been considered to overcome ISI caused by multipath propagation.

In the proposed system for full-duplex SIC, it is assumed that the Self and Far nodes use real-valued equispaced comb-type pilot patterns with the same subcarriers with index p as shown in Figure 1.

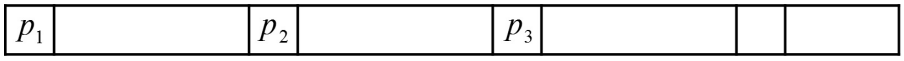

Figure 1. Pilot pattern.

Pilot vector $X_p = \left[P_1, P_2, \ldots, P_{N_p}\right]^T$ with the length N_p has been used for both Self and Far nodes.

At the Self node part, after the combination of data X_d at index d and pilot X_p at index p, the data X_S were created. Then, data X_S passed through IFFT and cyclic prefix blocks and $x_{S_{cp}}$ has been obtained. By using a similar way, $x_{F_{cp}}$ has been obtained at the Far node part. These two signals are subsequently sent through the SI and communication channels. The following subsection shows the model of SI and far channels.

3.2. The model of the channel

We construct a propagation channel model in this subsection, assuming a typical shallow water setting with water column level d_W shown in Figure 2.

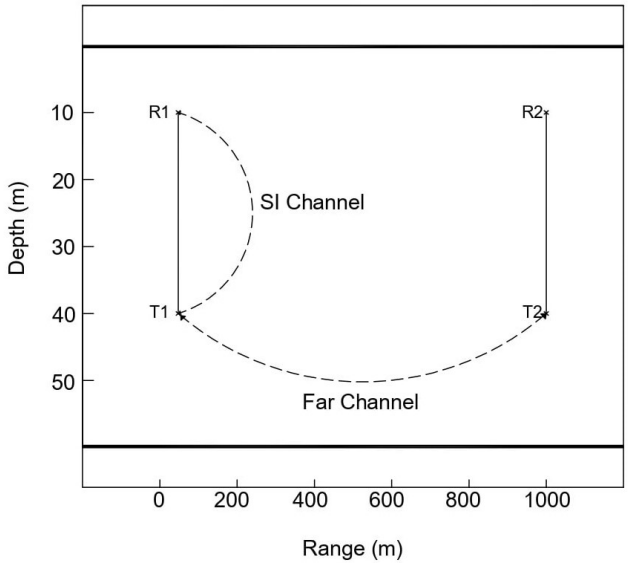

Figure 2. An acoustic IBFD shallow water communication system.

The two transmitted signals pass through their separate channels, indicated by the SI channel and Far channel, respectively. The UWA channel has a significant impact on the performance of the IBFD underwater wireless communication system. Due to the strong self-interference and multipath propagation, reliable information about the SI and communication channels are required to develop SI cancellation strategies successfully.

3.2.1. Far channel model

Characterising the propagation delay, spreading loss, transmission loss, and absorption loss of the vertical channel is essential for developing a fundamental model of the channel. Distance-related weakening of signal strength is expressed as a decibel (dB) value called transmission loss (TL). Attributable to a combination of

spreading loss and attenuation, it is quantified by [18]. The latter is what would happen if the sound was transmitted and immediately converted into heat due to friction.

$$\mathrm{TL}\,(f) = 2\alpha_z + k\,\log_{10}(r) + a\,(f)\,r, \tag{2}$$

where α_z denotes the 15 dB attenuation in the zy and zx planes. This is due to the fact that both the transducer and the receiver employ toroidal transducers with a beam pattern, r represents the propagation range in meters, and k is the spreading factor, which is 10 for spherical spreading and 20 for free-field spreading. In this computation, a practical law that lies between both the spherical and cylindrical laws is selected. The presence of magnesium sulphate in saltwater begins to contribute extra attenuation at frequencies lower than 500 kHz. Despite its low quantity in saltwater, boric acid contributes at frequencies lower than 700 Hz, and the equations that follow are related to the computation of $\alpha(f)$ where:

$$\alpha(f) = \alpha_1 + \alpha_2 + \alpha_3, \tag{3}$$

$$\text{(Freshwater attenuation) } \alpha_1 = af^2, \tag{4}$$

$$\text{(MgSO}_4\text{Relaxation) } \alpha_2 = b\,f_0/(1 + (f_0/f)^2), \tag{5}$$

$$\text{(Boric acid relaxation) } \alpha_3 = c\,f_1/(1 + (f_1/f)^2), \tag{6}$$

$$a = 1.3 \times (10 * \exp(-7)) + 2.1 \times ((10 * \exp(-10))\,(T - 38)^2, \tag{7}$$

$$b = 2S \times (10 * \exp(-5))\,, \tag{8}$$

$$c = 1.2 \times 10^{-4}, \tag{9}$$

$$f_0 = 50 \times (T + 1), \tag{10}$$

$$f_1 = (10)^{(T-4)/100}, \tag{11}$$

where $S = 35$ represents salinity in h, $T = 14$ means temperature in degrees of Celsius, and f=12 kHz indicates frequency band.

To model the communication channel between the self and far nodes, we propose a geometry model to represent the multipath propagation in the Far channel based on a triangle by setting the angle between the FD modem direction and water column $\theta = 90°$. Direct path propagation delay T_D is determined by using the velocity formula:

$$T_D = (D_T - D_R)/c, \tag{12}$$

where the transmitter depth, denoted by D_T, and the reception depth, indicated by D_R and $c = 1500$ means the sound speed. This model posits that D_R is not constant, and its value varies with respect to D_T. As seen in Figure 3, the angle $\theta = 90°$ is between a column of water and the FD direction.

$$D_R = D_T - L * \cos(\theta)\,, \tag{13}$$

where the distance L is separated between the transmitter and receiver. According to Figure 3, the delay in the propagation between the transmitter and the receiver may be calculated using the Pythagorean theorem of right triangles, whether the signal is traveling over a straight path or multipath. In this case, the hypotenuse reflects the time it takes for each reflection to complete its propagation. There are two sorts of assumed reverberations: surface reflections, in which the initial reflection occurs on the surface, and bottom reflections, in which the initial reflection occurs on the seafloor.

According to the Pythagorean theorem in a vast triangle, S constitutes d_1, which shows the propagation range by the initial reflection between the transmitter and the surface (the magnitude of the vertical motion on

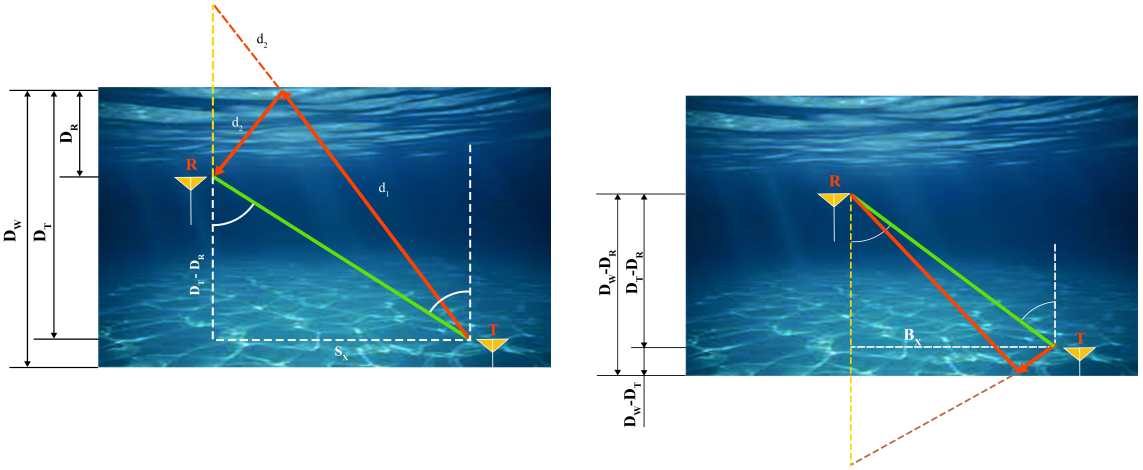

(A). Surface reflections. (B). Bottom reflections.

FIGURE 3. Multipath reflections in Far channel.

the first reflection line segment is equal to D_T) and then to the receiver, d_2 (the magnitude of the vertical motion on the second reflection line segment is equal to D_R) after drawing the reflected distance, d_2 is supplied to d_1 as an extension. So the sum of the vertical motion on these two line segments d_1 and d_2 is equal to $D_T + D_R$. The side indicated by S_y is perpendicular to the hypotenuse, while the side indicated by S_x is next to it.

$$S = \sqrt{{S_x}^2 + {S_y}^2} \tag{14}$$

$$S_y = D_T + D_R \tag{15}$$

$$S_x = (D_T + D_R) \tan\theta \tag{16}$$

For every number of surface reflections, n, between 1 and N, the propagation delay is calculated as:

$$S_{y_n} = D_T + \left[\frac{n}{2}\right] 2D_W + (-1)^{n+1} D_R, \tag{17}$$

where D_W is the water depth.

$$T_{Sn} = \left(\sqrt{(D_T + D_R)^2 \tan^2\theta + \left(D_T + \left[\frac{n}{2}\right] 2D_W + (-1)^{n+1} D_R\right)^2}\right)/c \tag{18}$$

The same method is used to calculate the time taken for a single bottom reflection to propagate. As illustrated in Figure 9 and the corresponding equation, B_x is unaffected by the number of reflections, whereas B_y does change.

$$B = \sqrt{{B_x}^2 + {B_y}^2} \tag{19}$$

$$B_y = D_T + D_R \tag{20}$$

$$B_x = (D_T - D_R) \tan\theta \tag{21}$$

For every number of bottom reflections, n, between 1 and N, the propagation delay is calculated as:

$$B_{y_n} = \left[\frac{n}{2}\right] 2D_W - \left(D_T + (-1)^{n+1} D_R\right) \tag{22}$$

The propagation delay for any number of reflections is computed depending on the velocity formula:

$$T_{Bn} = \left(\sqrt{(D_T - D_R)^2 \tan^2 \theta + \left(\left[\frac{n}{2} \right] 2D_W - \left(D_T + (-1)^{n+1} D_R \right) \right)^2} \right) / c \tag{23}$$

For normal incidence waves at the ocean's surface boundary, the pressure reflection coefficient is around -1, whereas for waves reflected off the ocean floor, it is roughly 1. Reflections from surfaces that are evenly spaced contribute positively at the receiver, whereas reflections from uneven surfaces or the bottom negatively.

Figure 4 shows the Far channel response of the multipath between the source and the receiver. The delay spread of the echoes in the Far channel was as high as 79 ms because of the multipath propagation. This is because the arrival times, amplitudes, and phases of signals change depending on the lengths of their original signal routes and the delay spread. Intersymbol interference is caused by the delayed receiver copies; hence, the propagation delay of the multipath compared to the direct path is an important feature of the underwater channel.

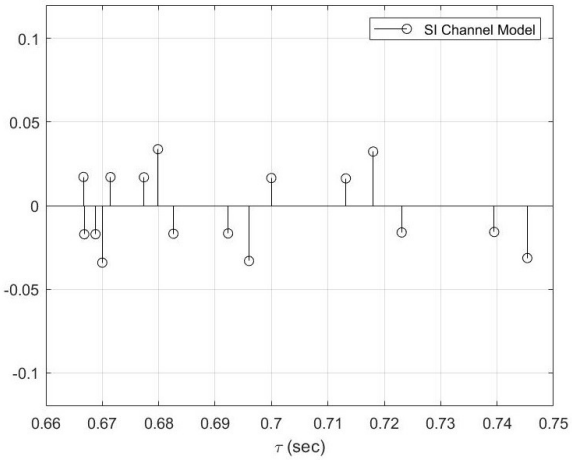

Figure 4. Far magnitude CIR with L=1000.

The Bellhop simulator [19] is used to evaluate the effectiveness of the proposed model with the same configuration parameters (D_W, D_R, D_T, L, f) as shown in Figures 5a and 5b, where the red path indicates a direct path or a signal that originates at the sea floor and refracts or diverges upwards until it encounters a steep positive sound speed gradient at which point it refracts downwards. By reflecting off of the water's surface and/or bottom, the signal may make its way to the receiver via the water's green route. In this case, the black routes indicate an increase in multipath components at the receiver as a result of a more significant number of potential paths reflected off of the sea surface and the uneven sea bottom. Results are relatively comparable when comparing the delay spread of the suggested model (79 ms) to those of the Bellhop simulator [19] (78 ms).

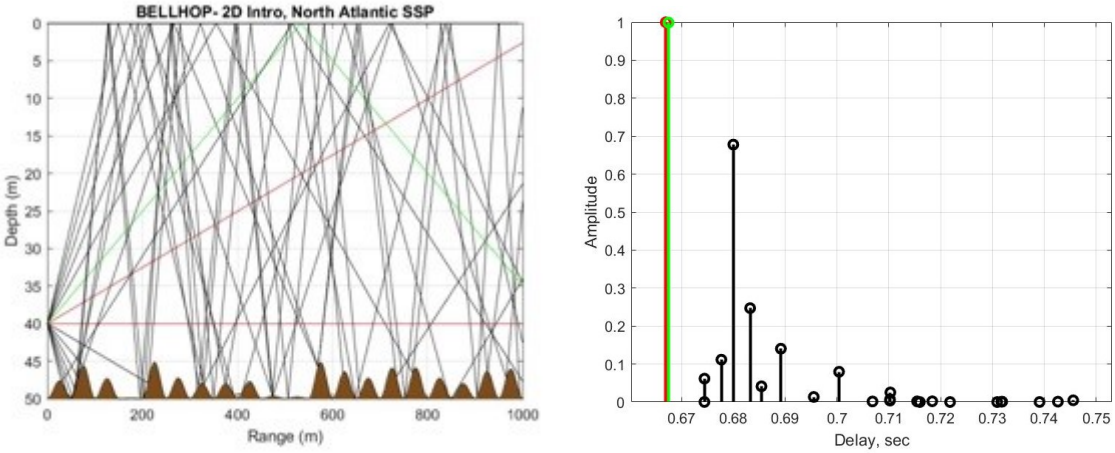

(a). Ray trace. (b). CIR.

Figure 5. Bellhop's multipath propagation setting in underwater.

3.2.2. SI CHANNEL MODEL

The channel coefficients and the magnitude channel impulse response, in seconds, for the Self node are generated based on the proposed modelr [20]. Due to the fluid nature of the marine environment, including the movement of organisms and ships, the FD may be displaced from the vertical direction at varying angles with the water column.

This research assumes two situations to describe a self-interference channel: one in which the angle between the water column and the FD direction is 0 degrees and another in which it is 4 degrees, as seen in Figure 6.

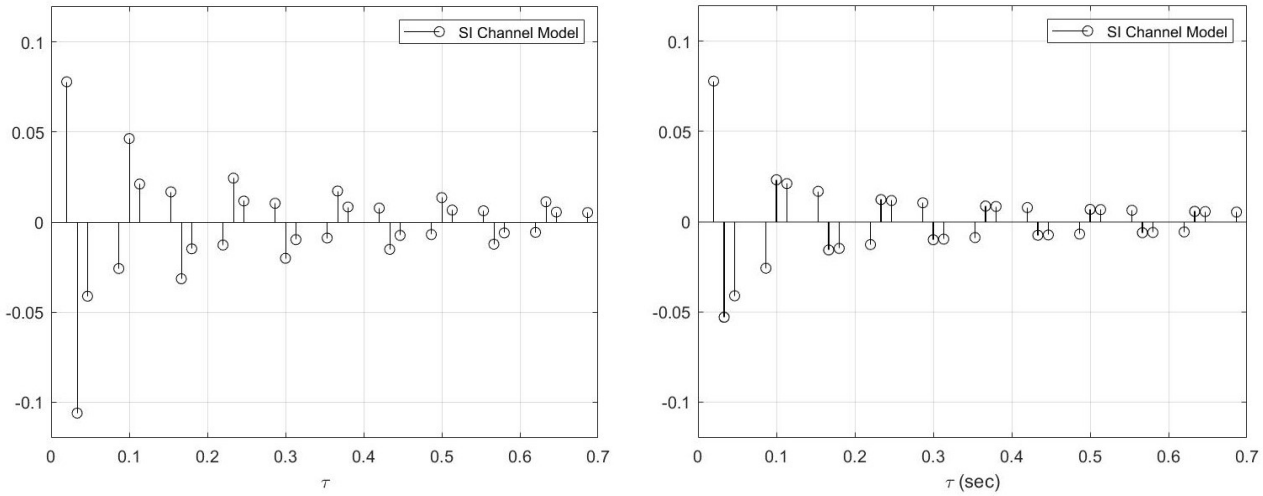

(A). $\theta = 0°$. (B). $\theta = 4°$.

FIGURE 6. SI magnitude CIR with L=30.

3.3. STRUCTURE OF THE RECEIVER

In this section, we propose a model that can remove self-interference in a full-duplex system by separating the Self signal from the Far signal. As mentioned previously, the two transmitted signals pass through their separate channels denoted SI channel and Far channel, respectively, and the summation of them with AWGN noise is received by the receiver antenna of the Self node, $\boldsymbol{r_{cp}}$ as shown in Figure 7.

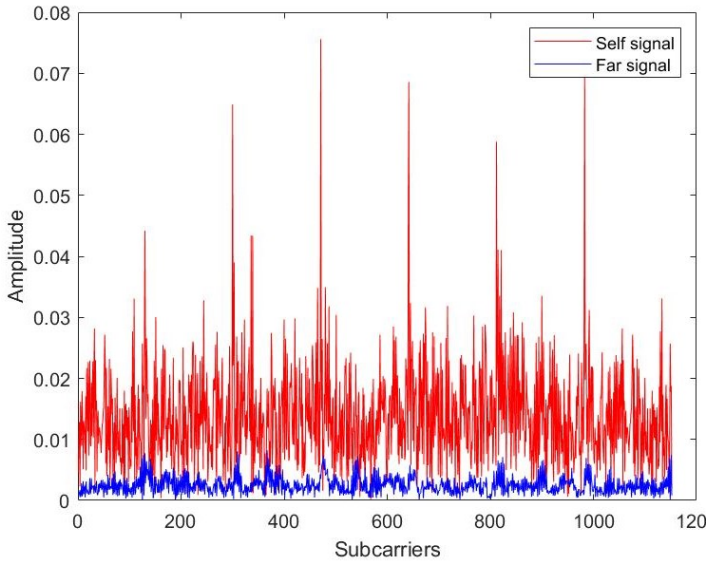

FIGURE 7. Received signals.

After removing the cyclic prefix and getting FFT from the received signal r_{cp} as illustrated in Figure 8, with an indication to number of subcarriers at each block, we have:

$$R = \tilde{X}_S H_S + \tilde{X}_F H_F + \mathcal{N}. \tag{24}$$

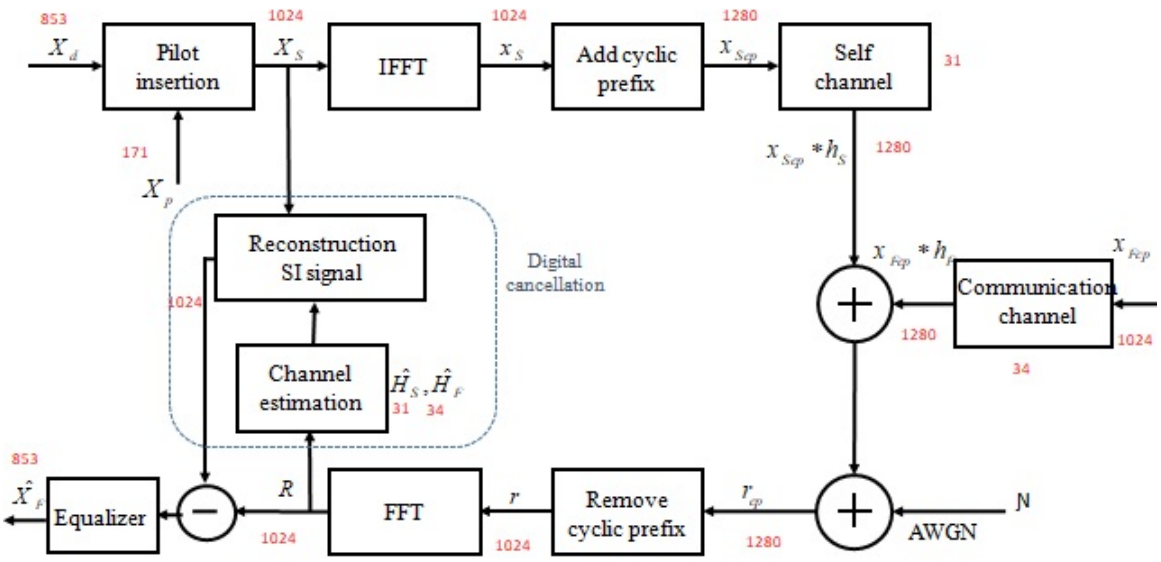

Figure 8. Structure of SIC-based OFDM IBFD-UWA communication system.

Whose $\tilde{X}$ referred to the diagonal matrix created by X.

$$X = [X_1, X_2, \ldots, X_N]^T$$
$$\tilde{X} = \begin{bmatrix} X_1 & 0 & 0 & 0 \\ 0 & X_2 & 0 & 0 \\ 0 & 0 & \ddots & \vdots \\ 0 & 0 & \ldots & X_N \end{bmatrix} \tag{25}$$

The proposed system assumed that the Self and Far channels are fixed for two OFDM blocks, and the Self node uses the pilot vector X_p for the first OFDM block, same as the Far node, but it uses $-X_p$ as the pilot vector for the second OFDM block, unlike the Far node that uses the same X_p as the first block. So we have

$$\begin{aligned} R_1 &= \tilde{X}_{S_1} H_S + \tilde{X}_{F_1} H_F + \mathcal{N}_1, \\ R_2 &= \tilde{X}_{S_2} H_S + \tilde{X}_{F_2} H_F + \mathcal{N}_2. \end{aligned} \tag{26}$$

In matrix form, we have

$$\begin{bmatrix} R_1 \\ R_2 \end{bmatrix} = \begin{bmatrix} \tilde{X}_{S_1} & \tilde{X}_{F_1} \\ \tilde{X}_{S_2} & \tilde{X}_{F_2} \end{bmatrix} \begin{bmatrix} H_S \\ H_F \end{bmatrix} + \begin{bmatrix} \mathcal{N}_1 \\ \mathcal{N}_2 \end{bmatrix} \tag{27}$$

If only pilot subcarriers for two received OFDM blocks R_1 and R_2 have been chosen, we have

$$\begin{bmatrix} R_{p_1} \\ R_{p_2} \end{bmatrix} = \begin{bmatrix} \tilde{X}_p & \tilde{X}_p \\ -\tilde{X}_p & \tilde{X}_p \end{bmatrix} \begin{bmatrix} H_{pS} \\ H_{pF} \end{bmatrix} + \begin{bmatrix} \mathcal{N}_{p_1} \\ \mathcal{N}_{p_2} \end{bmatrix} = A \begin{bmatrix} H_{pS} \\ H_{pF} \end{bmatrix} + \begin{bmatrix} \mathcal{N}_{p_1} \\ \mathcal{N}_{p_2} \end{bmatrix} \tag{28}$$

The matrix A is a $2N_p \times 2N_p$ real-valued unitary matrix [], $A^T A = I$, so the channel frequency response (CFR) of Self and Far channels in pilot subcarriers can be estimated by:

$$\begin{bmatrix} \hat{H}_{pS} \\ \hat{H}_{pF} \end{bmatrix} = \begin{bmatrix} \tilde{X}_p & \tilde{X}_p \\ -\tilde{X}_p & \tilde{X}_p^T \end{bmatrix}^T \begin{bmatrix} R_{p_1} \\ R_{p_2} \end{bmatrix} \tag{29}$$

With an interpolation, Self, and Far CFRs, $\hat{H}_S$ and $\hat{H}_F$ are estimated and because $\tilde{X}_{S_1}$ and $\tilde{X}_{S_2}$ are known by the Self node we have; therefore, SI $\hat{X}_{F_1}$ and $\hat{X}_{F_2}$ can be obtained by

$$\begin{bmatrix} \hat{X}_{F_1} \\ \hat{X}_{F_2} \end{bmatrix} = \tilde{\hat{H}}_F^{-1} \left(\begin{bmatrix} R_1 \\ R_2 \end{bmatrix} - \begin{bmatrix} \tilde{X}_{S_1} \\ \tilde{X}_{S_2} \end{bmatrix} \hat{H}_S \right) \tag{30}$$

In the proposed system, it can be seen that at the Self node, the separation of two Self and Far signals has been done completely, and SI cancellation from the Far node signal is made perfectly.

4. Simulation results

In this section, the simulation results of the proposed method for full-duplex systems will be discussed. The proposed orthogonal self-interference cancelation method based on mathematical proofs has no restrictions on the channel characteristics and all the channels that can be used in the OFDM system can be used in the proposed full-duplex system. Therefore, the proposed method for eliminating self-interference from Far signal is independent of the number of channel taps unlike method of [17], where the orthogonality condition is satisfied only in a certain number of channel taps.

Of course, similar to other communication systems, the characteristics of the channel, the length of the channel impulse response, the number of pilots used for the channel estimation and the type of the method used for channel estimation will be important and influential for the channel estimation efficiency of the proposed system and the MSE and BER curves, but it will not have any effect on the main goal of the proposed paper, which is the complete and accurate removal of self-interference signal from the Far signal.

All simulations are done in MATLAB based on the system model shown in the Figure 8 and Table 1 and the simulation results are the average of 1000 simulation repetitions. In the following figures, the efficiency of the proposed method for self-interference cancelation and channel estimation is well illustrated by MSE and BER parameters.

Parameter	**Value**
Bandwidth B	6 kHz
Number of sub-carrier Nc	1024
Signal constellation	QPSK
CP interval	256 (1024/4)
Carrier frequency	12 kHz
Sampling frequency	48 kHz
Pilot arrangement	Comb type

Table 1. Simulation parameters.

In the following figures, the simulation results of the proposed self-interference cancelation method for full-duplex systems are shown based on establishing orthogonality between two Self signals and Far signals in different modes and the efficiency and performance of the proposed system have been evaluated.

As shown in Figure 9, the MSE curve of the Far channel estimation in the two modes of the proposed full-duplex and the conventional half-duplex completely coincide, and this figure shows the accuracy and efficiency of the proposed method, which results in the correct separation of the Self and Far channels that is obtained based on orthogonality and is the main goal and contribution of this paper. In the MSE curves, the estimation efficiency of the Self channel is better than that of the Far channel because the Self channel has better conditions due to the proximity of the transmitter and receiver.

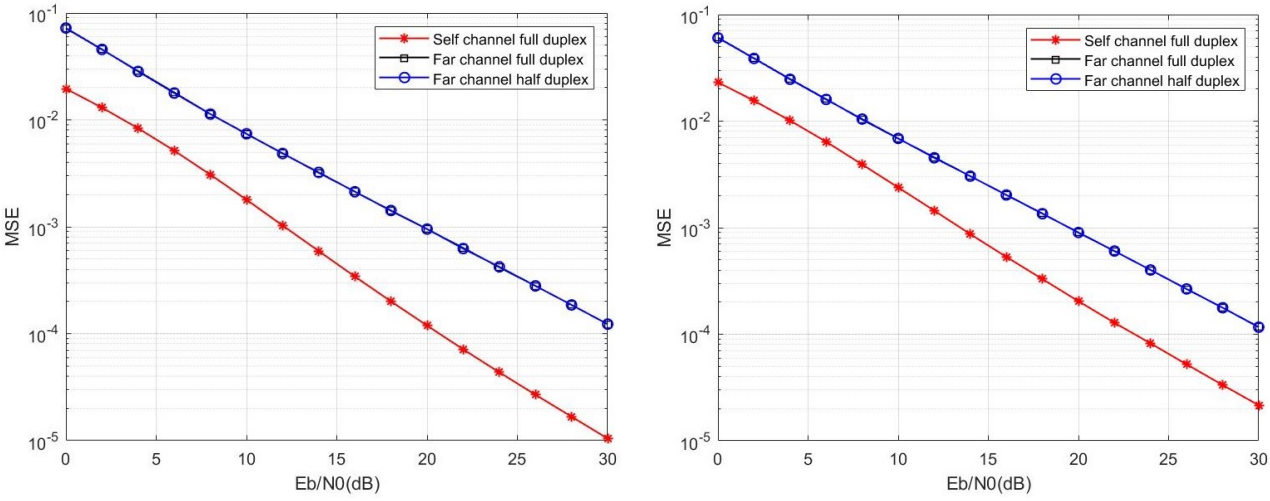

(a). $\theta = 0°$. (b). $\theta = 4°$.

Figure 9. MSE of the MMSE channel estimation at different angles.

In Figure 10, the BER curves for two full-duplex and half-duplex systems are illustrated. It can be seen that the two curves are not exactly identical and there is a slight difference between them. But this difference is inevitable and is not the reason for the inefficiency of the proposed method. According to the BER curve, the performance of the half-duplex system is slightly better than the full-duplex system, which is related to the overall structure of the full-duplex system.

In the half-duplex system, the Far channel is first estimated, then the Far data are extracted. But in the full-duplex system, in general, the Self channel is estimated first. Then the product of the estimated Self channel by the Self data is calculated and is subtracted from the received data. Finally, according to the data obtained from the previous step, the Far channel is estimated and the Far data are extracted, according to equation 30 (of course, in the proposed method, due to the existence of orthogonality, both Self and Far channels are estimated simultaneously). That is why the bit error efficiency of the half-duplex system is slightly better than that of the full-duplex system. Of course, it should be mentioned again that the bandwidth usage of the full-duplex system is twice that of the half-duplex system.

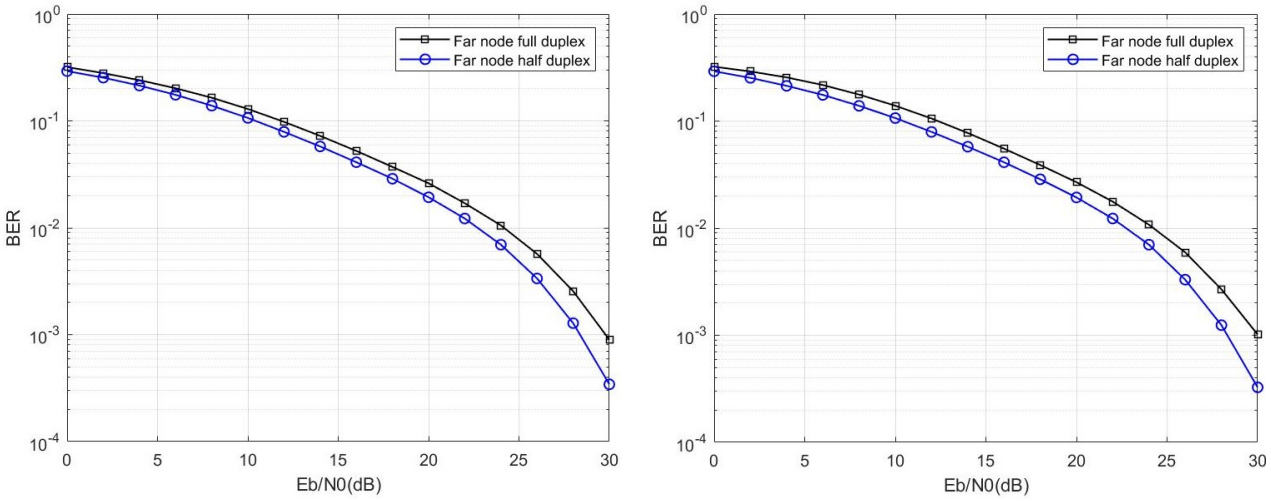

(A). $\theta = 0°$. (B). $\theta = 4°$.

FIGURE 10. BER of the MMSE channel estimation at different angles.

In Figure 11 and Figure 12, the MSE and BER curves were displayed using the MMSE channel estimation method for different channels with different channel lengths. As can be concluded from these figures, the proposed method for cancelling self-interference has no limitations and is suitable for each channel with different characteristics. Also, we can see from Figure 13 and Figure 14 that the proposed orthogonal full-duplex method has a high efficiency in dealing with different Self-node and Far-node distances, and changes in the distance do not affect the system's efficiency.

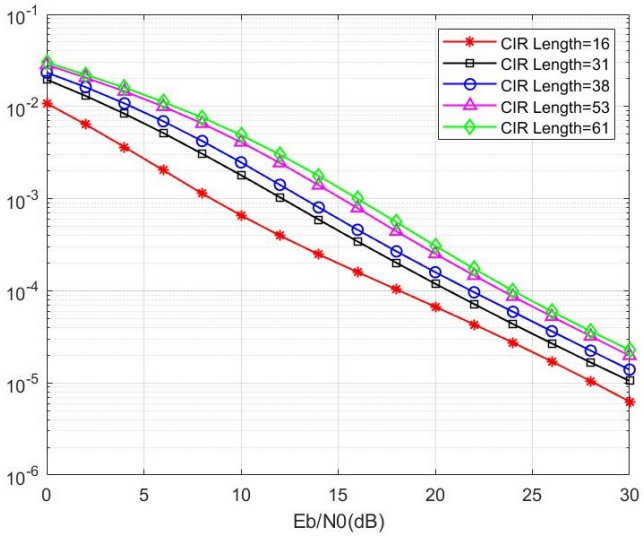

FIGURE 11. MSE of the SI MMSE channel estimation with different CIR length.

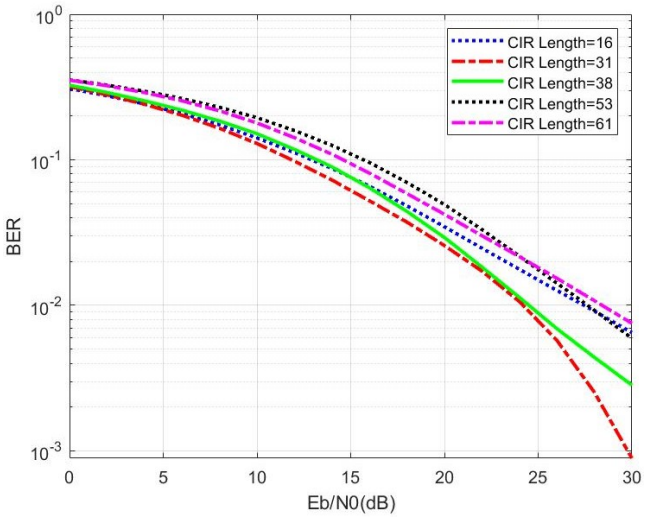

FIGURE 12. BER of the Far MMSE channel estimation with different CIR length.

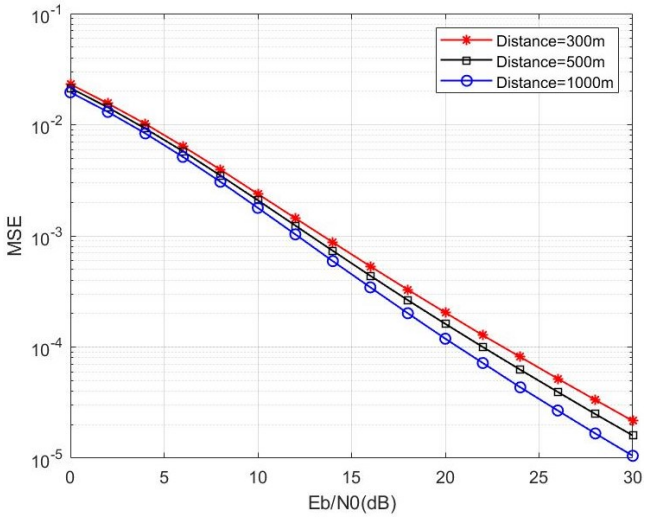

FIGURE 13. MSE of the SI MMSE channel estimation with different distances.

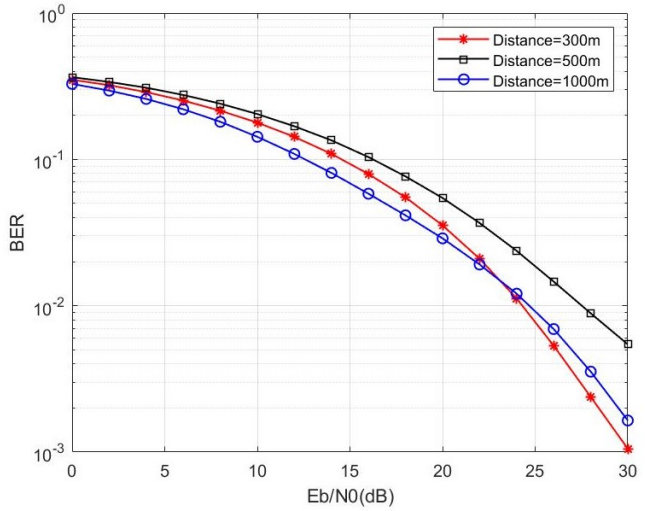

FIGURE 14. BER of the Far MMSE channel estimation with different distances.

Finally, Figure 15 shows the actual and estimated channel frequency response for both the Self-channel and the Far-channel. As can be seen, the channel estimation accuracy is excellent in both channels, and this is due to the accurate separation of the two Self signal and Far signal. In the proposed system, by establishing orthogonality conditions between two signals, the estimation of both channels occurs simultaneously and the elimination of self-interference is done effectively, which is a big problem in full-duplex systems, and the proposed method of this paper can be a suitable solution of this problem.

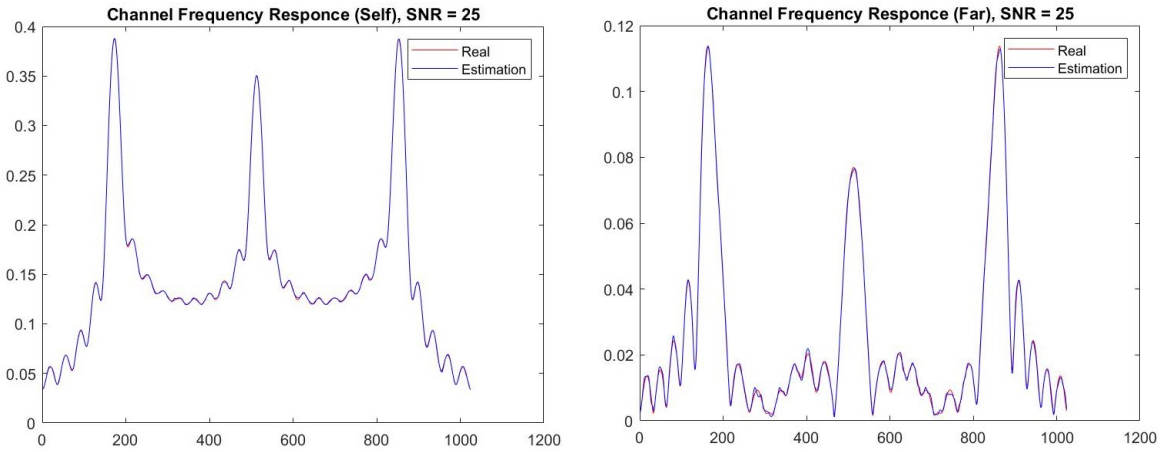

(a). Self channel. (b). Far channel.

Figure 15. Estimation of CFR.

5. Conclusion

In this paper, the separation of Self signal from Far signal in full-duplex systems is presented. The proposed self-interference cancelation method uses two received OFDM blocks and provides orthogonality between the Self signal and the Far signal, and in this way separates the Far signal from the self-interference signal. The main contribution of this paper is the complete and accurate cancelation of self-interference from the Far signal without the conditions of the Self and Far channels affecting the efficiency of the proposed method, unlike previous works that had these problems. The correctness of the proposed method has been proved mathematically and it has been shown by a simulation and comparison with the half-duplex system that the efficiency of channel estimation and receiving Far-node data in the proposed full-duplex system are the same as that of the half-duplex system. It is also shown that the proposed method has a good performance with fixed or shifted FD and no dependence on the channel length or distance. As a result, the proposed method can be considered a good solution for full-duplex systems with much better spectral performance than half-duplex systems. The findings also indicate that the proposed channel model correctly represents the behaviour of multipath propagation in a shallow water environment in a delay spread as compared with the traditional works in horizontal communications, where the results at $\theta = 90°$are very close with Bellhop simulator for delay spread measurement.

References

[1] M. Stojanovic, J. Preisig. Underwater acoustic communication channels: Propagation models and statistical characterization. *IEEE Communications Magazine* **47**(1):84–89, 2009. https://doi.org/10.1109/MCOM.2009.4752682

[2] A. E. Abdelkareem, B. S. Sharif, C. C. Tsimenidis, J. A. Neasham. Compensation of linear multiscale Doppler for OFDM-based underwater acoustic communication systems. *Compensation of Linear Multiscale Doppler for OFDM-Based Underwater Acoustic Communication Systems* **2012**:139416, 2012. https://doi.org/10.1155/2012/139416

[3] M. C. Domingo. Overview of channel models for underwater wireless communication networks. *Physical Communication* **1**(3):163–182, 2008. https://doi.org/10.1016/j.phycom.2008.09.001

[4] Z. Zhang, K. Long, A. V. Vasilakos, L. Hanzo. Full-duplex wireless communications: Challenges, solutions, and future research directions. *Proceedings of the IEEE* **104**(7):1369–1409, 2016. https://doi.org/10.1109/JPROC.2015.2497203

[5] K. E. Kolodziej, B. T. Perry, J. S. Herd. In-band full-duplex technology: Techniques and systems survey. *IEEE Transactions on Microwave Theory and Techniques* **67**(7):3025–3041, 2019. https://doi.org/10.1109/TMTT.2019.2896561

[6] G. Qiao, S. Liu, Z. Sun, F. Zhou. Full-duplex, multi-user and parameter reconfigurable underwater acoustic communication modem. In *2013 OCEANS – San Diego*, pp. 1–8. 2013. https://doi.org/10.23919/OCEANS.2013.6741096

[7] J. Zhang, G. Qiao, C. Wang. Acoustic communication networks. In *2013 OCEANS – San Diego*, pp. 1–6. 2013. https://doi.org/10.23919/OCEANS.2013.6741129

[8] L. Shen, B. Henson, Y. Zakharov, P. Mitchell. Digital self-interference cancellation for full-duplex underwater acoustic systems. *IEEE Transactions on Circuits and Systems II: Express Briefs* **67**(1):192–196, 2020. https://doi.org/10.1109/TCSII.2019.2904391

[9] L. Li, A. Song, L. J. Cimini, et al. Interference cancellation in in-band full-duplex underwater acoustic systems. In *OCEANS 2015 - MTS/IEEE Washington*, pp. 1–6. 2015. https://doi.org/10.23919/OCEANS.2015.7404411

[10] Y. Widiarti, Suwadi, Wirawan, T. Suryani. A geometry-based underwater acoustic channel model for time reversal acoustic communication. In *2018 International Seminar on Intelligent Technology and Its Applications (ISITIA)*, pp. 345–350. 2018. https://doi.org/10.1109/ISITIA.2018.8711067

[11] J. Zhou, H. Jiang, P. Wu, Q. Chen. Study of propagation channel characteristics for underwater acoustic communication environments. *IEEE Access* **7**:79438–79445, 2019. https://doi.org/10.1109/ACCESS.2019.2921808

[12] X. Zhu, C.-X. Wang, R. Ma. A 2D non-stationary channel model for underwater acoustic communication systems. In *2021 IEEE 93rd Vehicular Technology Conference (VTC2021-Spring)*, pp. 1–6. 2021. https://doi.org/10.1109/VTC2021-Spring51267.2021.9448976

[13] S. Panchal, S. Patel, S. Panchal, J. Pabari. Design of novel channel propagation model for underwater acoustic wireless communication inside a tank. *Research Square* 2022. https://doi.org/10.21203/rs.3.rs-1842984/v1

[14] G. Qiao, S. Gan, S. Liu, Q. Song. Self-interference channel estimation algorithm based on maximum-likelihood estimator in in-band full-duplex underwater acoustic communication system. *IEEE Access* **6**:62324–62334, 2018. https://doi.org/10.1109/ACCESS.2018.2875916

[15] M. Shammaa, H. Vogt, A. El-Mahdy, A. Sezgin. Adaptive self-interference cancellation for full duplex systems with auxiliary receiver. In *2019 International Conference on Advanced Communication Technologies and Networking (CommNet)*, pp. 1–8. 2019. https://doi.org/10.1109/COMMNET.2019.8742358

[16] Z. S. Liu, Q. J. Zhou, W. S. Gan, et al. Adaptive joint channel estimation of digital self-interference cancelation in co-time co-frequency full-duplex underwater acoustic communication. In *2019 IEEE International Conference on Signal, Information and Data Processing (ICSIDP)*, pp. 1–5. 2019. https://doi.org/10.1109/ICSIDP47821.2019.9173156

[17] A. M. M. Chandran, L. Wang, M. Zawodniok. Channel estimators for full-duplex communication using orthogonal pilot sequences. *IEEE Access* **8**:117706–117713, 2020. https://doi.org/10.1109/ACCESS.2020.3002726

[18] R. F. W. Coates. *Underwater acoustic systems.* Macmillan, 1990. https://doi.org/10.1007/978-1-349-20508-0

[19] N. Morozs. Channel modeling for underwater acoustic network simulation, 2020. P. 1–25. https://doi.org/10.24433/CO.1789096.v1

[20] H. A. Naman, A. E. Abdelkareem. Variable direction-based self-interference full-duplex channel model for underwater acoustic communication systems. *International Journal of Communication Systems* **35**(7):e5096, 2022. https://doi.org/https://doi.org/10.1002/dac.5096